THE LOCALIZATION OF TRANSPORT PROPERTIES IN THE FROG LENS

RICHARD T. MATHIAS, JAMES L. RAE, LISA EBIHARA, AND RICHARD T. MCCARTHY
Department of Physiology, Rush Medical College, Chicago, Illinois 60612

ABSTRACT The selectivity of fiber-cell membranes and surface-cell membranes in the frog lens is examined using a combination of ion substitutions and impedance studies. We replace bath sodium and chloride, one at a time, with less permeant substitute ions and we increase bath potassium at the expense of sodium. We then record the time course and steady-state value of the intracellular potential. Once a new steady state has been reached, we perform a small signal-frequency–domain impedance study. The impedance study allows us to separately determine the values of inner fiber-cell membrane conductance and surface-cell membrane conductance. If a membrane is permeable to a particular ion, we presume that the conductance of that membrane will change with the concentration of the permeant ion. Thus, the impedance studies allow us to localize the site of permeability to inner or surface membranes. Similarly, the time course of the change in intracellular potential will be rapid if surface membranes are the site of permeation whereas it will be slow if the new solution has to diffuse into the intercellular space to cause voltage changes. Lastly, the value of steady-state voltage change provides an estimate of the lens' permeability, at least for chloride and potassium. The results for sodium are complex and not well understood. From the above studies we conclude: (*a*) surface membranes are dominated by potassium permeability; (*b*) inner fiber-cell membranes are permeable to sodium and chloride, in approximately equal amounts; and (*c*) inner fiber-cell membranes have a rather small permeability to potassium.

INTRODUCTION

One of the many important functions of epithelia is to regulate the composition of the compartments that they line. To do so, the transport properties of apical and basolateral membranes must differ. These differences may be in the types of active or coupled transport systems or in the selectivity of the membranes for passive ion flux. Thus, the spatial localization of membrane transport properties is essential to the function of most epithelia and characterization of this localization is one of the main goals of epithelial research.

The lens is an atypical epithelial tissue with a unique geometry and no obvious role in the overall ocular transport system. Nevertheless, when one looks carefully at the electrical, physiological, or structural properties of the lens, it is apparent that its transport properties are highly localized. Fig. 1 is a sketch of a lens cut in cross section to illustrate the localization of structural properties. The anterior surface is covered with a monolayer of cuboidal epithelial cells, whose membranes can be classified as either apical or basolateral. The posterior surface and equatorial zone are comprised of immature fiber cells (differentiating epithelial cells), and the mass of the lens is comprised of mature fiber cells. All of these cells are electrically interconnected through low-resistance gap junctions (Benedetti et al., 1976; Goodenough, 1979; Goodenough et al., 1980; Mathias et al., 1981; Rae and Kuszak, 1983, and other papers reviewed in Rae and Mathias, 1984). Because of the syncytial structure of the lens, it is difficult to separately study the electrical properties of the different cell types. Nevertheless, a number of studies have demonstrated that transport properties are indeed localized.

Electrophysiological and histochemical studies of Kinsey and Reddy (1965), Palva and Palkama (1974), Kinoshita (1963), and Neville et al. (1978) have shown that the Na/K pumps in the lens are predominantly located in the lateral membranes of the anterior epithelium, but some are also found in the membranes of immature fiber cells. Candia et al. (1971), Delamere and Duncan (1979), and Platsch and Wiederholt (1981) each used an Ussing chamber to demonstrate anterior/posterior asymmetries in the passive and active transport properties of lens membranes. Mathias et al. (1979) used impedance techniques to demonstrate a large difference in the membrane conductance of inner mature fiber cells and and other surface cells. Robinson and Patterson (1983) used a vibrating probe to demonstrate standing, steady-state current loops through the lens.

All of the above studies suggest that there is a high degree of spatial localization of transport properties within the lens, yet we have little information on the distribution of passive transmembrane flux. To a first approximation, we can classify the localization as: (*a*) surface vs. inner membrane; and (*b*) anterior vs. posterior surface mem-

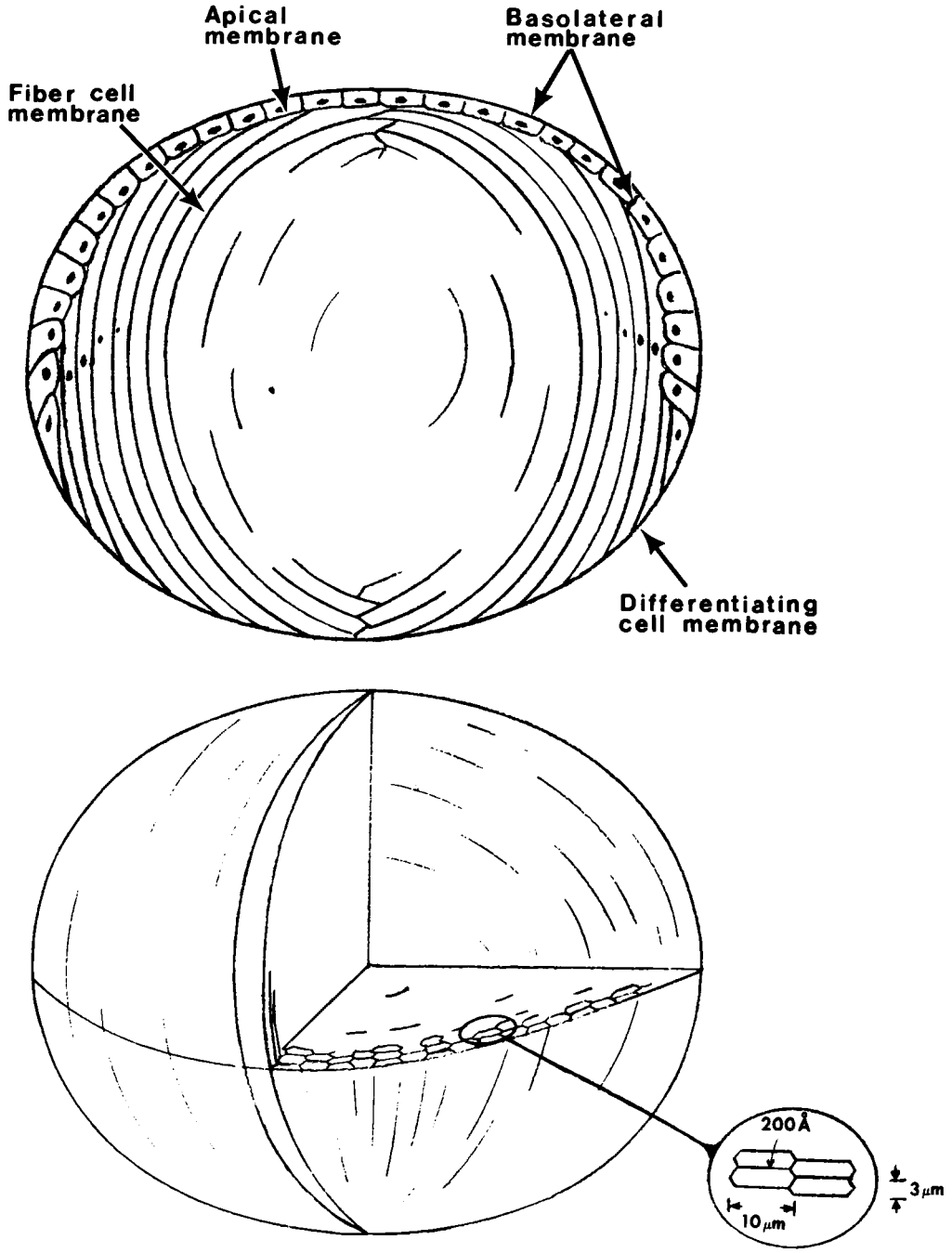

FIGURE 1 A diagram of structural specializations within the lens. The anterior surface is covered with a single layer of cuboidal epithelial cells. The apical membranes of these cells face the small restricted extracellular space between epithelial and fiber cells; the lateral membranes face the lateral intercellular space of the epithelium; and the basal membranes face the bath. At the equator, the epithelial cells begin to elongate and differentiate into fiber cells. The immature fiber cells lose their intracellular organelles as they become internalized to the lens by newer cells growing on top of them. The posterior ends of these immature fiber cells are foot-like and pack together to form the posterior surface of the lens. The vast majority of the lens is comprised of mature fiber cells, which have no intracellular organelles and whose membranes all face the small intercellular space within the lens.

brane, though there are certainly other more detailed specializations likely to be present around the epithelium and equator. The spatial distribution of resting voltage within the frog lens has a distinct radial gradient (Rae, 1974*a*, *b*; Taura et al., 1979; Mathias and Rae, 1985), thus surface vs. inner localization of properties seems to be important in this preparation. The purpose of this paper is to provide the first crude estimates of the selectivity of inner and surface membranes in the frog lens. In the companion paper (Mathias, 1985), we examine some of the physiological consequences of the radial localization of properties described here.

THEORY

The impedance data were compared with the spherical syncytium model derived by Eisenberg et al. (1979), as modified by Mathias et al. (1981) to include radial nonuniformity in cell-to-cell coupling. To a first-order approximation, the input impedance is given by the parallel combination of the surface membrane admittance, Y_S, and the input admittance to the intercellular clefts, y_e, in series with the convergence resistance, R_S, due to the point source of current being injected into a cell at the lens' center.

$$Z = R_S + \frac{1}{4\pi a^2 (Y_S + y_e)} + o(\epsilon), \qquad (1)$$

where

$$Y_S = G_S + j\omega C_S,$$

$$y_e = \frac{\gamma}{R_e}\left(\coth \gamma a + \frac{1}{\gamma a}\right),$$

$$\gamma^2 = (R_e + R_i)\frac{S_m}{V_T}(g_m + j\omega c_m),$$

$$R_S = \frac{1}{4\pi}\left(\frac{1}{r} - \frac{1}{a}\right), \qquad r_1 \le r \le a,$$

$$R_S = \frac{1}{4\pi}\left(\frac{1}{r} - \frac{1}{r_1}\right)\alpha R_i + \frac{1}{4\pi}\left(\frac{1}{r_1} - \frac{1}{a}\right) R_i, \; 0 \le r \le r_1, \qquad (2)$$

and the small $o(\epsilon)$ correction terms are described in Mathias et al. (1981).

The basic building blocks for the model are described in the Glossary.

The first-order approximation assumes that g_m, R_e, and S_m/V_T are radially uniform and that G_S is the average of any angular nonuniformities in the surface membrane conductance. If there are small (order ϵ) radial nonuniformities, then g_m, R_e, and S_m/V_T represent the radial average of the parameter and small correction terms must be added to the $o(\epsilon)$ component of the impedance. If there are large radial nonuniformities, the theory is inaccurate.

GLOSSARY

a	lens radius (cm)
c_m	specific capacitance of the inner fiber cell membranes (F/cm^2)
C_S	specific capacitance of the surface cell membranes (F/cm^2)
g_m	specific conductance of the inner fiber cell membranes (S/cm^2)
G_S	specific conductance of the surface cell membranes (S/cm^2)
r	radial location of the voltage recording microelectrode (cm)
r_1	radial location at which the effective intracellular resistivity changes from αR_i to R_i (cm)
S_m/V_T	surface of membrane per unit volume of tissue (cm^{-1})
R_e	effective extracellular resistivity (Ω cm)
R_i	effective intracellular resistivity (Ω cm)
α	ratio of the effective intracellular resistivity in the nucleus, $r \le r_1$, to that in the cortex, $r \ge r_1$.
ϵ	small parameter used in the perturbation expansion of Eisenberg et al. (1979), $\epsilon \approx R_i/(R_i + R_e)$.

METHODS

Electrophysiology

Small grass frogs (*Rana pipiens*) were killed and the lenses dissected in accordance with procedures described in Mathias et al. (1979). The lenses were mounted in a small chamber by pinning the attached uveal-scleral ring to the Sylgard-lined bottom of the chamber.

Two intracellular microelectrodes were placed in the lens, one in the center to pass current, the other ~200 μm beneath the posterior surface to record voltage. A small wide-band stochastic current was injected and recorded: the induced voltage (~2 mV peak to peak) was also recorded; the recorded voltage and current were sent to a Fourier Analyzer (model 5420A; Hewlett-Packard Co., Palo Alto, CA) where the impedance was calculated in real time. The shielding of microelectrodes, details of recording the impedance and calibration procedure for the electrode time constants are described in Mathias et al. (1981).

Curve Fitting

The Hewlett-Packard Co. Fourier analyzer produces the magnitude and phase of the impedance at 256 frequency points, which are linearly spaced between 0 Hz and the chosen maximum frequency. We curve fit to data at 200 frequency points, which are approximately equally spaced on a log frequency scale between 0.08 and 800 Hz. To obtain the necessary density of points on a log scale, we used three separate Hewlett-Packard Co. files, which have maximum frequencies of 12, 100, and 800 Hz. We arbitrarily chose 200 points as a compromise that provides an adequate density of points, yet does not require excessive computational time in the curve-fitting procedure. Wild points usually occur at multiples of the line frequency and these are removed from the data; other than the wild point editing, no smoothing (i.e., neighboring point averaging) is done.

The data are compared to the model (Eq. 1) and a nonlinear curve-fitting algorithm (Levenberg-Marquardt, IMSL, Inc., Houston, TX) was used to extract the best-fit parameter values. In determining the average parameter values presented in Table II, six parameters were varied in the curve-fitting procedure: G_S, C_S, g_m, c_m, R_i, and R_e. In an experiment where the composition of the bathing solution was varied, we first varied all six parameters in fitting the data in the different solutions; we then determined the average values of C_S and c_m and refit the data with the capacitances fixed at their average value. This procedure reduced the variability due to correlation between parameters (see the Discussion for an expanded description of this procedure).

Solutions

The chamber used in these experiments was ~10 mm in diameter and the depth of solution was generally ~4 to 5 mm. New solutions were applied by rotating a hydraulic switch (Altex-Beckman Instruments, Irvine, CA) that was connected to several different solutions. Each solution was driven through the switch by gravity flow and the level of the bath was maintained constant by a surface outflow port connected to a vacuum bottle. The switch was mounted ~1 cm from the bath. This position minimized the amount of dead volume that needed to be changed when a new solution was applied. The time to completely change the composition of the bath in this system was ~3 s, as estimated by observation of dye washout. However, the small intercellular spaces within the lens are an unstirred compartment, and the composition of the solution within this compartment will not come to diffusional equilibrium with the bath until many minutes after the bath has reached steady state (Rae et al., 1982).

All lenses were initially bathed in our normal Ringer's solution for this preparation (concentrations are given in millimoles per liter): Na^+ = 107, K^+ = 2.5, Ca^{++} = 2, Cl^- = 114, $H_2PO_4^-$ = 0.4, and HPO_4^- = 0.9, with pH = 7.3. In all of our ion substitutions, the pH, ionic strength, and osmolarity of the bath were maintained constant while we substituted a relatively impermeant ion for the permeant ion of interest. Table I lists the concentrations of Na^+, K^+, and Cl^- that were used in the impedance studies. The normal Ringer's solution is marked NR; the solution in which we make the minimum change in the ion of interest (test ion) is marked ΔMIN; the solutions in which we make the next-greatest and greatest changes in the test ion are marked ΔMED and ΔMAX, respectively. When Cl^- was reduced, we substituted methanesulfonate ($MeSO_4^-$); when K^+ was increased Na^+ was reduced; when Na^+ was reduced, we substituted tetramethylammonium (TMA^+). Other ion substitutions

TABLE I
ION SUBSTITUTIONS

Test Ion	NR	ΔMIN	ΔMED	ΔMAX
Cl^-	114	90	50	23
K^+	3	5	15	30
Na^+	107	100	80	60

The concentration of the substitute ion is given by the concentration change in the test ion from its value in normal Ringer's solution (NR).

were tested and are mentioned in the Results, but for a variety of reasons the effects of these other substitutions were not sufficiently specific to warrant a quantitative analysis.

In each ion substitution experiment, we performed the protocol described in the Results in the presence and absence of 100 μm ouabain. The ouabain was added to the solutions described in Table I with no attempt to adjust osmolarity.

RESULTS

General

Table II presents the average parameter values from all of the lenses used in these studies. The values in Table II are derived from impedance data recorded in NR. The variation from lens to lens in the derived values of G_S and g_m is at least as great as the changes in these parameters reported in Figs. 2, 4, 6, and 8. Thus, in tabulating the subsequent figures, we first normalize the conductance to its value in NR, then average the fractional change in conductance from each lens. The standard errors in Table II therefore represent the lens to lens variability in conductance whereas the standard error bars in Figs. 2, 4, 6, and 8 represent the variability in the effect of the solution change.

Specific Protocol

Our protocol is based on the idea that if a membrane is permeable to a particular ion, then the conductance of the membrane should vary with the concentration of that ion (Hodgkin and Katz, 1949). We replace both Na^+ and Cl^- to varying extents with larger ions, which should be much less permeant, or we increase bath K^+ at the expense of Na^+, then we study the impedance of the lens in these replacement solutions. The impedance protocol allows us to quantitatively estimate the conductance of inner fiber-cell membranes separately from the conductance of surface-cell membranes, thereby providing an estimate of the site of permeability.

The intercellular clefts within the lens are just a few hundred angstroms in width, yet they extend from the surface to the center. Estimates of the effective diffusion constant for the intercellular spaces have been made based on impedance data (Rae et al., 1982) and measurement of diffusion of radioactive tracers (Paterson and Maurice, 1971). From these experiments, one expects the intercellular clefts to come to a reasonable diffusional equilibrium with the bath in ~1 hr. The intracellular compartment is isolated from the clefts by the cell membranes, hence one expects significant changes in intracellular concentration to require a much longer time. For example, if we assume that about one-half g_m is due to sodium channels and if we could immediately change the transmembrane sodium gradient by ΔE_{Na}, then the initial rate of sodium accumulation in the cells is given by $(S_m/V_T)(g_m/2)(\Delta E_{Na}/F)$. For ΔE_{Na} of 15 mV and the value of g_m in Table II, the initial rate of intracellular accumulation would be ~0.1 mM/h. We therefore waited ~1 h between solution changes since we felt that this was long enough to change the intercellular solution but short enough to avoid significant changes in the intracellular solution.

The upper graph in Fig. 2 illustrates a typical protocol. We impale the lens with two microelectrodes at $t = 0$, then wait 1 h to make sure the lens is not running down or there is some other problem. We make our first impedance study in NR at $t = 1$ h, then we change to our next solution, which is the ΔMIN in Table I. We wait for the new solution to diffuse into the intercellular spaces of the lens, then make a second impedance study at $t = 2$ h and change to the ΔMED solution, and so on. Sometimes the lens would be damaged during the course of this long protocol, so we always went through the sequence of solution changes NR-ΔMIN-ΔMED-ΔMAX-ΔMED-ΔMIN-NR. We considered the experiment successful when the final input resistance in our last NR solution was 80% or more of the original value. If the lens had been damaged during the protocol, the input resistance in the final NR solution was usually <50% of the original value. It is worth noting that the intracellular resting voltage always recovered to near its original value, even when the input resistance indicated severe damage.

TABLE II
AVERAGE PARAMETER VALUES IN NORMAL RINGER'S SOLUTION FOR THE 24 LENSES USED TO COMPILE FIGURES 2, 4, 6, AND 8

	G_S (mS/cm²)	C_S (μF/cm²)	g_m (μS/cm²)	c_m (μF/cm²)	R_e (KΩ-cm)	R_i (KΩ-cm)	a (cm)	ψ_i (mV)
Mean	28.9	3.13	0.464	0.80	52.3	2.92	0.157	−74
±SEM	1.8	0.88	0.088	0.05	3.2	0.15	0.003	1

Other parameters in the model were set as follows: from Mathias et al. (1979) $S_m/V_T = 6{,}000\ cm^{-1}$; from Mathias et al. (1981) $r_1 = 0.65a$ and $\alpha = 2.4$. The values of a, ψ_i, and $r = 0.137$ cm were directly measured; the remainder of the parameters were determined by curve fitting the model to impedance data.

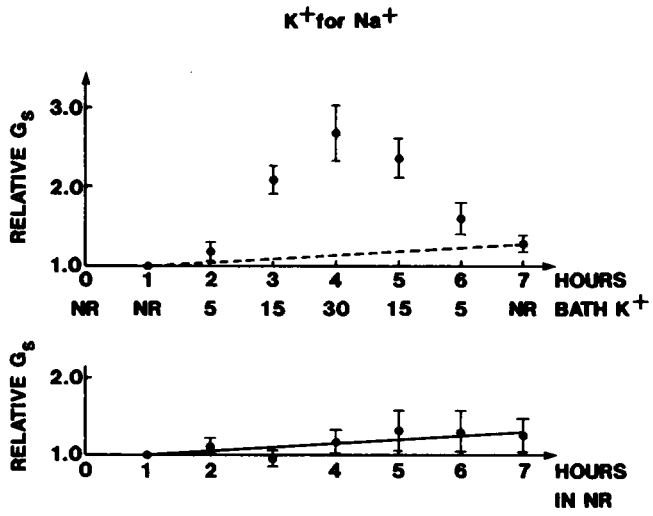

FIGURE 2 The time-dependent run down in surface membrane conductance as measured by impedance studies: *upper* panel shows a typical protocol for systematically changing the concentration of a permeant ion (in this case potassium) and the resulting conductance increases due to both concentration dependence and time dependence (11 lenses ± SD); the *lower* panel shows the time dependent run down when there are no changes in the composition of the bath (three lenses ± SD).

The above described protocol is lengthy and one cannot expect living tissue to remain in perfect health, particularly when impaled with two electrodes and frequently buffeted by solution changes. Thus, what one considers unacceptable damage is a matter of judgment. In our best experiments, the input resistance recovered to some 95% of its original value, and as mentioned above in the worst experiment we report, the input resistance recovered to at least 80% of its original value.

Even if one does not subject the lens to abnormal bathing media, the input resistance always falls to some extent with time and this is illustrated in the bottom graph of Fig. 2. Accordingly, we cannot believe small systematic conductance increases unless we demonstrate that the conductance change really depends on concentration of the test ion and not on time. To control for the time-dependent rundown of resistance, we only accepted experiments in which the above-described protocol was completed. We would then average the values of conductance recorded at t = 1 h in NR and t = 7 h in NR. Similarly, we averaged the t = 2 h ΔMIN conductance with the t = 6 h ΔMIN conductance; and we average the t = 3 h ΔMED conductance with the t = 5 h ΔMED conductance. The t = 4 h ΔMAX conductance is recorded halfway through the experiment and is therefore assumed to intrinsically include the average time dependent run down. These averaged values of conductance from one lens were then averaged with similar results from other lenses and Figs. 4, 6, and 8 were constructed.

Chloride Changes

We used a protocol similar to that illustrated in Fig. 2 to put the lens through a sequence of four solutions containing varying amounts of Cl^-. The impedance was recorded in each solution. Fig. 3 illustrates the lens impedance in NR and in the lowest chloride concentration we studied. The smooth curves represent the fit of our model to the data.

When the concentration of Cl^- in the bath was reduced, there was a small systematic increase in the input resistance of the lens. This can be seen in the magnitude plot shown in Fig. 3. Presumably, the chloride substitute methanesulfonate ($MeSO_4^-$) is not permeant, whereas chloride is permeant, hence the reduction in the concentration of permeant ions causes the membrane resistance to increase. As the input resistance of the lens increased, a noticeable change appears in the phase delay of the impedance. This can be seen in Fig. 3 in the frequency range of 1 to 10 Hz. In order for the model to account for these changes in the impedance, the value of g_m had to be dropped considerably, whereas no other parameter needed to be changed.

Fig. 4 *A* summarizes the average changes observed in the four different chloride solutions. The value of the inner membrane conductance falls to perhaps one-half its normal value in the lowest chloride solution indicating that perhaps one-half of the inner membrane conductance is for chloride. The smooth curve connecting the values of g_m was arbitrarily drawn to indicate our perception of the trend. Note that the value of G_S does not vary significantly as chloride is removed, hence we conclude there is little or no chloride conductance at the surface. The value of intracellular voltage, ψ_i, also systematically depolarized as chloride was removed. The steady-state changes illustrated in Fig. 4 *A* are consistent with about one-half of g_m being chloride

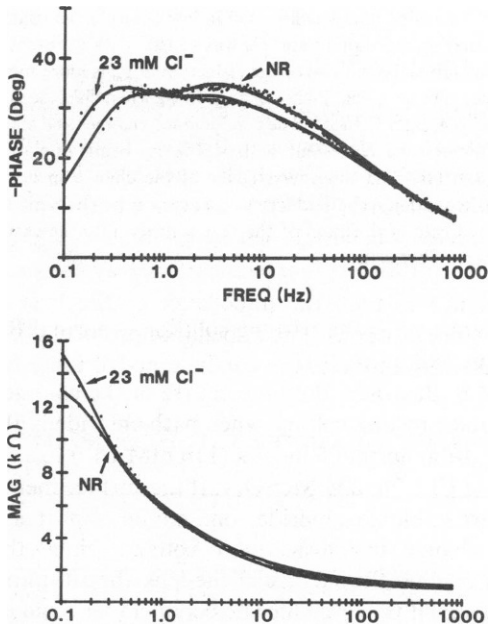

FIGURE 3 The impedance of the frog lens in NR solution and in low chloride (Cl^- = 23 mM) with methanesulfonate ($MeSO_4^-$ = 91 mM) substituted for chloride.

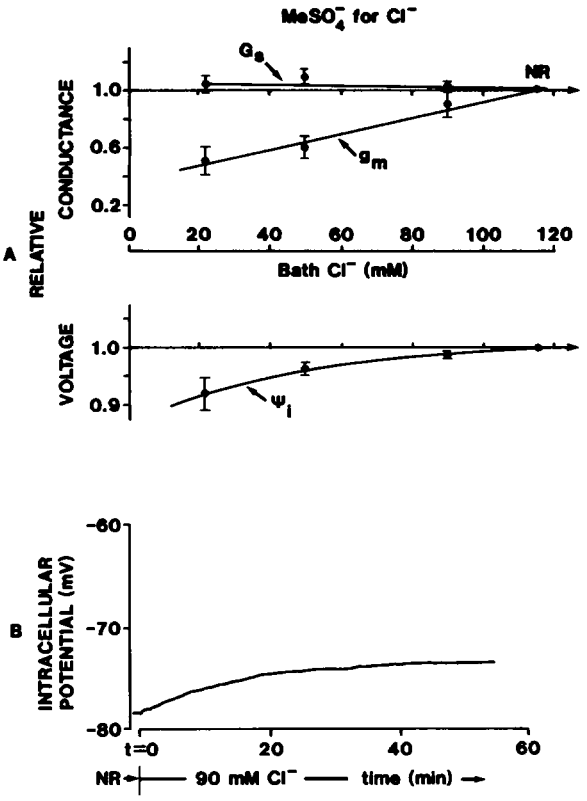

FIGURE 4 Conductance changes and changes in the steady state intracellular potential that occur in response to reducing bath chloride. The values are calculated by averaging out the time dependence in accordance with the procedure illustrated in Fig. 2. The conductances and voltages are from five lenses ± SEM, whose radius was >0.15 cm. In six other experiments on lenses whose radius was <0.12 cm, we obtained qualitatively the same result, except that in small lenses the inner membranes contribute relatively less importantly to the input impedance (relative to surface membranes) and the curve-fitting procedure was not sensitive enough to determine how much g_m fell in low chloride: we could only be confident that g_m was falling and G_S was constant. We present only the large lens result since the size of the reduction in g_m is more meaningful. There appears to be no significant change in G_S when chloride is removed whereas g_m is greatly reduced. The conductance changes and steady-state voltage changes are consistent with ~50% g_m being due to chloride permeability. (*B*) The time dependence of the change in intracellular voltage on reduction of bath chloride. The slow time course is typical of the expected rate of diffusion of the new solution into the extracellular clefts between fiber cells.

conductance when the bathing solution is normal Ringer's (Mathias, 1985; Eq. 38).

Fig. 4 *B* illustrates the time course of the change in the intracellular resting voltage when bath chloride is abruptly changed from normal Ringer's (114 mM Cl^-) to a solution of 90 mM Cl^-, 24 mM $MeSO_4^-$. If the surface membranes were permeable to chloride, one would expect a rather abrupt change in intracellular voltage, since the new solution reaches the surface of the lens almost immediately. However, if the lens chloride conductance resides in the inner-fiber cell membranes, then one would expect the gradual depolarization illustrated in Fig. 4 *B*, since the time course for the new solution to diffuse between the cells and throughout the extracellular compartment will be slow (Rae et al., 1982; Paterson and Maurice, 1971).

We therefore have three independent lines of evidence suggesting the chloride permeability of the lens resides on inner membranes; (*a*) the site of conductance changes; (*b*) the steady-state value of intracellular voltage change; and (*c*) the time course of the intracellular voltage change.

Potassium Changes

To increase the concentration of bath potassium but keep the osmolarity constant, it is necessary to reduce the concentration of sodium. Hence potassium changes could not be conducted as cleanly as the chloride substitutions and the effects described here reflect changes in both Na and K. However, a 12-fold increase in K^+ requires only a 28% reduction in Na^+, thus we believe the changes we observe are dominated by the effect of increasing potassium.

Fig. 5 illustrates the large change in lens impedance when bath potassium is increased to the ΔMAX K^+ concentration of 30 mM. The input resistance falls to less than one-half of its original value, indicating a large conductance increase with the increase in potassium. Because the lens obviously has a relatively large selectivity for potassium, the increase in K^+ causes depolarization that may induce further increases in conductance (Patmore and Duncan, 1980).

We conducted some experiments in which a voltage clamp circuit was used to control the intracellular voltage, but of course one cannot control the transmembrane voltage in a syncytium comprised of hundreds of thousands of cells packed together with intercellular spaces on the

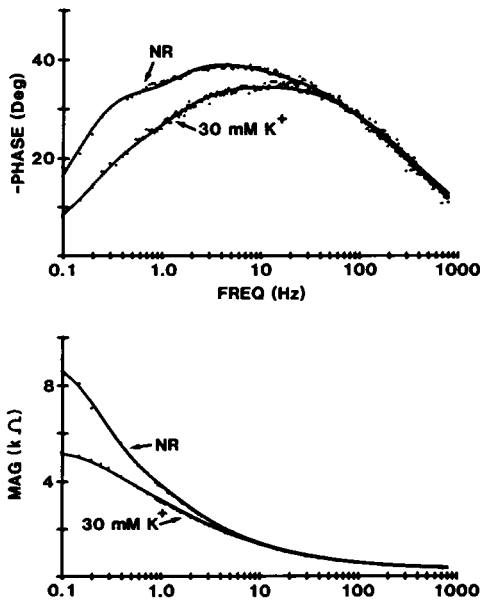

FIGURE 5 The impedance of the frog lens in NR and high potassium (K^+ = 30 mM) with reduced sodium (Na^+ = 77 mM).

order of 100 Å (Attwell et al., 1979; Johnson and Lieberman, 1971). Although there appears to be some voltage dependence to the membrane conductances in the lens, the major rectification in the current-voltage relationship usually occurred about the steady-state intracellular voltage, regardless of its value. In other words, the major rectification appeared to be current dependent, and probably reflected accumulation/depletion of ions induced by the large steady current. A similar observation was made by Delamere et al. (1980), though they did not consider accumulation/depletion of intercellular ions. We concluded that voltage clamp studies would not be useful in sorting out voltage- vs. concentration-dependent conductance changes, so the potassium substitution results presented here include both.

Fig. 6 *A* shows the enormous increase in our derived value of surface-membrane conductance, G_S, that occurs when bath potassium is increased. This suggests a large potassium permeability at the surface.

The conclusions concerning the inner membrane conductance, g_m, are not so clear. We believe a significant fraction of the conductance g_m is due to sodium selective channels, but in order to increase potassium we had to decrease sodium. Thus, if g_m had no selectivity for potassium, one would expect a decrease in g_m due to the reduced sodium. However, the large potassium conductance at the lens surface has caused the lens to depolarize, and most channels open more frequently with depolarization (Rae and Levis, 1984; Rae, 1985), thus one would expect some increase in g_m due to the depolarization even if inner membranes had no potassium permeability. To further complicate the issue, g_m may include a small component of potassium conductance. However, if g_m included a large component of potassium conductance, one would expect the concentration change and the voltage change together to cause a large increase in g_m. Since the changes in the derived value g_m are small, we believe the selectivity of the inner membranes for potassium is small, whereas the surface membranes appear to be dominated by their potassium selectivity.

The large steady-state change in intracellular voltage shown in Fig. 6 *A* suggests the lens has a relatively large selectivity for potassium. The time course of the change in intracellular voltage following a change in bath potassium from 2.5 to 30 mM is illustrated in Fig. 6 *B*. The majority of the voltage change occurs very rapidly as the new potassium concentration rapidly reaches the surface membranes. There is then a small slower depolarization, which is faster than the chloride-induced depolarization shown in Fig. 4 *B*, but is too slow to be due to the mixing in the bath. One possible explanation for this slow change is that the fiber cells in the outer cortex of the lens have some potassium channels.

All of these results indicate the majority of the lens potassium channels reside in the surface membranes. The density of potassium channels on inner-fiber cell membranes appears to be quite low, and the few that do exist are probably close to the surface.

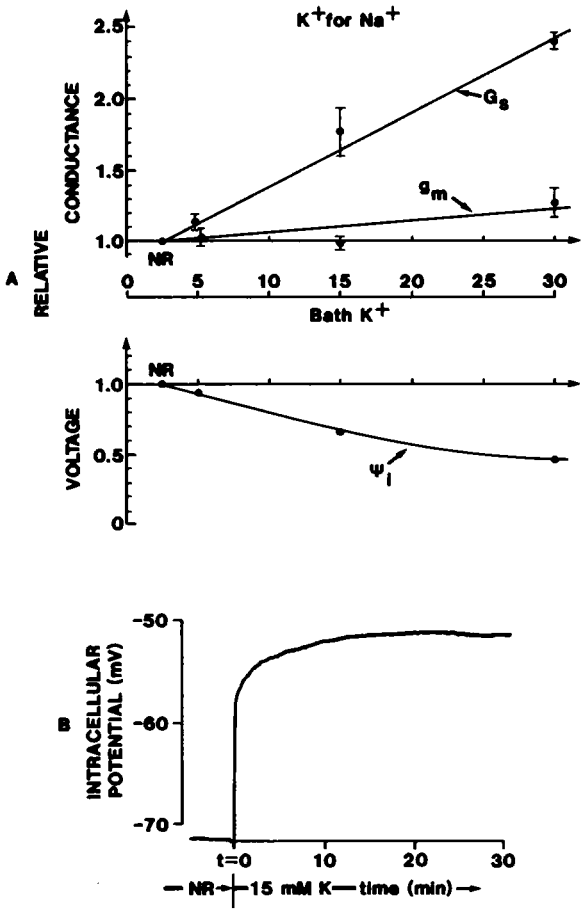

FIGURE 6 (*A*) Conductance changes and changes in the steady state intracellular potential that occur in response to increasing bath potassium. The values are calculated by averaging out the time dependence illustrated in Fig. 2. The conductances and voltages are from 11 lenses ± SEM. The changes in G_s and ψ_i are consistent with essentially 100% G_s being due to potassium permeability. The changes in g_m are small and may be due to changes in ψ_i rather than potassium. We conclude the potassium permeability of the fiber cell membranes is small. (*B*) The time dependence of the changes in ψ_i on substitution of 15 mM K^+ for Na^+. The initial, very rapid depolarization is consistent with the surface-cell membrane conductance, G_s, being dominated by potassium selectivity. The subsequent slower change may be due to some potassium permeability in the immature fiber cells, whose membranes face the restricted extracellular space but they are relatively near to the lens surface.

Sodium Changes

Of the experiments reported here, the results of removing sodium were the most difficult to obtain and are the most difficult to interpret. We presume that small frog lenses possess a significant resting sodium conductance since the intracellular voltage is at least 20 mV positive to E_K (Paterson et al., 1974) and since the lens is actively extruding sodium by an Na-K ATPase at the rate of ~20 p moles/s (Neville et al., 1978). Either of these observations suggest that some 20% of the input conductance is attribut-

able to sodium. The question we would like to answer is: Are the channels responsible for passive sodium permeation primarily located in inner-fiber cell membranes or surface-cell membranes?

We used a number of different sodium substitutes but none of them was totally satisfactory. The frog lens does not survive very well in reduced sodium; moreover, once sodium has been removed there is usually an irreversible, time-dependent rundown. We studied the effects of replacing sodium with (*a*) choline (Ch^+), (*b*) tetraethylammonium (TEA^+), and (*c*) tetramethylammonium (TMA^+). Furthermore, we performed two experiments in which cesium was substituted for sodium. Because of the above problems, the majority of these experiments will not be reported here. There was, however, one common theme to all of the sodium removal studies: if the time-dependent rundown was averaged out as described in Specific Protocol, then the value of the fiber-cell membrane conductance, g_m, always fell as sodium was reduced. The results for the surface-cell membrane conductance, G_s, were not consistent: when TEA^+ was substituted for Na^+, the time-independent (averaged) value of G_s fell slightly but the time-dependent rundown did not reverse; when TMA^+ was substituted, the averaged value of G_s increased slightly; when Ch^+ or cesium was substituted, the deterioration and variance precluded any conclusions. These results suggest a significant fraction of g_m is due to sodium permeability and we tentatively conclude the fraction of G_s attributable to sodium permeability is small.

The only sodium substitute that induced reversible changes was TMA^+. Fig. 7 shows the impedance in the initial NR solution and in the ΔMAX Na^+ solution containing 60 mM Na^+ and 47 mM TMA^+. We see that the input resistance of the lens reversibly falls when Na^+ is removed and TMA^+ is substituted. This would be the expected result if TMA^+ were more permeable than Na^+ or if TMA^+ has some pharmacological effect beyond that of low sodium.

Fig. 8 summarizes the reversible changes we observed in TMA^+ for Na^+ substitution experiments. The value of G_S increases in proportion to the concentration of TMA^+. The value of g_m falls with reduced sodium, and it increases as sodium is restored.

The change in intracellular voltage in response to reducing sodium turned out not to be useful in the localization of lens sodium selectivity. When sodium is reduced, the lens initially begins to hyperpolarize as one would expect, however, within ~1 min the lens begins to gradually depolarize and within 1 h it returns to near its original value. This behavior was observed with all sodium substitutes, in the presence or absence of ouabain. One possible explanation of our sodium substitution results is that low sodium turns on sodium permeable channels in the surface membranes. (A similar observation was reported by Fuchs et al., 1977, for frog skin.) In TMA^+ for Na^+, this effect appears to reverse in the frog lens but with the other

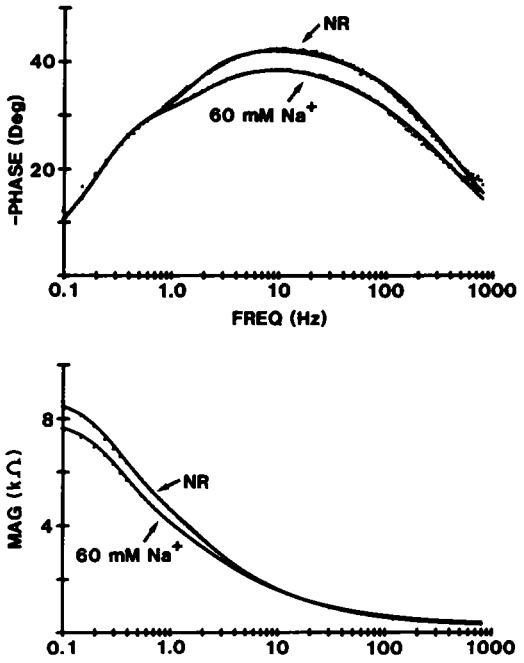

FIGURE 7 The impedance of the frog lens in NR solution and in low sodium (Na^+ = 60 mM) with tetramethylammonium (TMA^+ = 47 mM) substituted for sodium. The increase in conductance in low sodium may be due to a reversible pharmacological effect of TMA^+ on the surface membranes. See the discussion in the text.

substitutes the effect does not reverse, and in fact progresses with time (see the Discussion section on Sodium Permeability).

DISCUSSION

The experiments described in the previous section suggest the following general conclusions. (*a*) The chloride conductance of the lens is not large and is located almost exclusively in the membranes of mature fiber cells. (*b*) The surface cells have a membrane conductance that is dominated by potassium selectivity. (*c*) The mature fiber-cell membranes have a significant sodium selectivity. (*d*) The potassium selectivity of the fiber-cell membranes is small. (*e*) The sodium selectivity of surface cells is small in comparison to the potassium selectivity, and it probably does not represent a significant component of the total sodium conductance of the lens.

The above qualitatively described conclusions are quantitatively examined in the accompanying paper by Mathias (1985). Though the quantitative treatment does not prove the validity of the conclusions, it clearly shows that they are consistent with the known steady-state properties of the frog lens, such as resting voltage, the rate of active Na/K exchange, and the membrane conductances of surface and fiber cells. Moreover, Mathias and Rae (1985) and Taura et al. (1979) report the spatial distribution of steady state voltages recorded from the intracellular and intercellular spaces of frog lenses. The localization of selectivity described here accounts for the large recorded value of

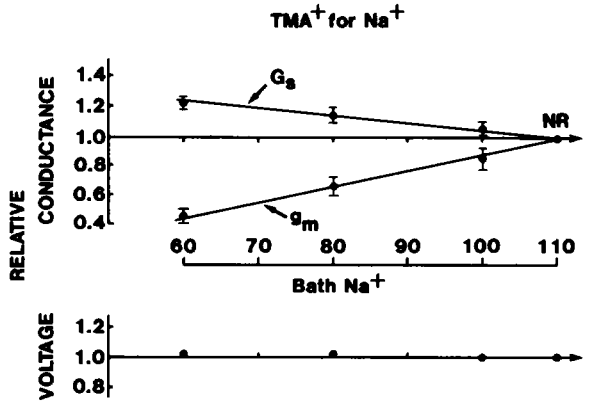

FIGURE 8 Conductance changes and changes in the steady-state intracellular potential that occur in response to reducing bath sodium and substituting TMA^+. The values are calculated by averaging out the time dependence in accordance with the procedure illustrated in Fig. 2. The conductances and voltages are from 11 lenses ± SEM. The large decrease in g_m consistently occurred with all sodium substitutes and suggests that ~50% g_m is due to sodium selectivity. The small increase in G_s in TMA^+ may be a reversible pharmacological effect. Other sodium substitutes did not necessarily cause a concentration-dependent increase in G_s, but they caused a time-dependent run down of G_s that was irreversible. The absence of steady-state voltage changes is not understood. There was a transient hyperpolarization, but within 15 min ψ_i returned to near its original value. Perhaps surface membrane channels are gated in response to sodium removal and these channels are permeable to sodium.

intercellular voltage as well as the spatial variation of the intercellular and intracellular potentials. This is particularly compelling evidence for the above conclusions, since the recorded standing radial voltage gradients imply circulating current and the above described separation of sodium and potassium permeabilities is needed to generate such a circulating current.

Parameter Value Estimation

Because the model in Eq. 1 is derived from the structure of the lens, it contains more parameters than can be determined by electrical measurements alone. Moreover, the curve fitting procedure is an indirect method of extracting parameter values and it is not possible to analytically predict the number of parameters that can be reliably determined. We have therefore performed extensive analysis and simulations to determine empirically which parameters in the model could be reliably determined, given the frequency resolution and noise in the data, as well as inadequacies of the model.

It can be shown that Eq. 1 and the auxillary definitions of terms will not represent a minimum equivalent circuit (i.e., a circuit that is, in principle, uniquely defined by its impedance), unless one specifies the values of a, r, and S_m/V_T. We directly measure the radius, a, and radial location of the voltage electrode, r, as described in Mathias et al. (1981). The surface of membrane per unit volume of tissue, S_m/V_T, is fixed at a value estimated from electron microscopic studies as described in Mathias et al. (1979). This leaves eight parameters: G_S, C_S, g_m, c_m, R_e, R_i, r_l, and α. If one records the impedance in the lens' cortex, $r > r_l$, as we have done in these studies, then α and r_l have only order ϵ effects on the theoretical impedance function (see Eq. 2). Hence, we have fixed α and r_l at their average values reported in Mathias et al. (1981), where we measured the impedance at numerous radial locations. The remaining six parameters can usually be determined by curve fitting; their average values in NR are reported in Table II.

Though each of the parameters reported in Table II has significant effects on the impedance function, some are loosely correlated with one another and the curve-fitting procedure can therefore produce similar fits with slightly different sets of parameter values (we estimate ±20% variability in the worst case). In previous papers and with regard to Table II, we have averaged parameter values from curve fits to data from many different lenses. We believe that the uncertainty in any particular set of parameter values is greatly reduced in the average values; moreover the biological variability considerably exceeds the uncertainty in a given experiment. Thus, average parameter values should not be affected by this sort of uncertainty, however, when we look for systematic changes in best fit parameters as the bathing solution is changed, the correlation of parameters becomes more of a problem.

In tabulating the conductance changes described in Figs. 4, 6, and 8, we first curve fit to all six parameters. The conclusions from this method of deriving the conductances were qualitatively identical to those presented, but the standard errors were much larger. We noted that the curve fitter produced slightly different values of membrane capacitance (±15%) in each solution. We assumed that the bathing solution should not affect the membrane capacitance, rather, we were seeing effects of noise in the data and correlation between parameters. We therefore calculated the average value of C_S and c_m for each lens and refit to the data in different solutions with the capacitances as fixed parameters. This procedure not only significantly reduced the standard errors, it also showed that almost every individual lens produced the same systematic changes in our derived values of conductance as we present for the average values.

The other parameters that were varied in this procedure were the effective intracellular resistivity, R_i, and the effective extracellular resistivity, R_e. We reasoned that some of the ion substitutes or pharmacological interventions might have long-term effects on intracellular pH, thereby causing some uncoupling of gap junctions and changing R_i. We also reasoned that some of our solution changes might cause small changes in cellular volume, thereby changing the spacing between cells and altering the value of R_e. For example, a 1% reduction in cellular dimensions is equivalent to a 500% increase in the dimensions of the intercellular spaces. Indeed, in some situations we observed small changes in either R_i or R_e. These

changes were sometimes complicated but they never appeared to affect our conclusions on localization of membrane conductance.

Chloride Permeability

Duncan (1970) and Guerschanik et al. (1977) studied the chloride permeability of toad and bullfrog lenses by observing the washout rate of radioactively labeled chloride. They concluded that the lens has a relatively large chloride permeability (compared with sodium) but, of course, this technique provided no information about the localization of transmembrane flux to inner vs. surface-cell membranes, nor does it distinguish between electrodiffusional flux and membrane transport. Moreover, Duncan (1970), Guerschanik et al. (1977), and Paterson (1971) all reported values for E_{Cl} that are significantly (+15 mV) positive to the intracellular resting potential, though no evidence for chloride transport was found.

The quantitative evaluation of our results presented in the subsequent paper (Mathias, 1985) and measurements of intercellular voltage (Rae, 1974*a*, *b*; Taura et al., 1977; Mathias and Rae, 1985) suggest there will be a large radial gradient in the extracellular voltage, with the voltage reaching 20 to 40 mV negative at the center of a small frog lens. Thus, the transmembrane voltage of the fiber cells, which is the intracellular minus the extracellular voltage, is on average significantly positive to the measured intracellular potential. Hence, our localization of chloride permeability to the fiber cell membranes requires that the Nernst potential, E_{Cl}, must on average be positive to the intracellular voltage, so the results of Duncan (1970), Paterson (1971), and Guerschanik et al. (1977) are consistent with our results and they do not necessarily imply active or exchange transport mechanisms for chloride.

The high chloride permeability of the lens suggested by the washout experiments may be due to electroneutral chloride exchange. However, it also seems likely that the radially circulating chloride flux calculated in the next paper (see Fig. 6 of Mathias, 1985) will greatly accelerate the exchange of intracellular chloride. Thus, the rapid washout of chloride may be due to circulation induced by the localization of properties described here rather than a high chloride permeability. In the lenses of the frog, mouse, rat, and chick, patch-clamp studies (Rae, 1985) have not yet found any chloride channels. Thus, we feel conclusion (*a*) of the Discussion is consistent with all of the data presently available on the lens chloride permeability.

Potassium Permeability

Duncan (1969) was the first to suggest that the potassium permeability of the lens is primarily localized near the surface. His conclusion was based on the rapid change in resting voltage on exposing the toad lens to a high potassium bath. Fig. 6 of this paper illustrates the time course of the voltage change in the frog lens on exposure to high potassium and, indeed, our data support Duncan's observation and conclusion. Moreover, whole-cell voltage-clamp studies of isolated frog lens epithelial cells (Rae, 1985) supports the dominance of potassium channels in these surface cells.

The amount of potassium permeability present in fiber cell membranes is more difficult to judge. Rae (1985) has found many nonselective cation channels in patch clamp studies of surface fiber cells of the frog lens. These channels pass either sodium or potassium with equal ease, hence the substitution of sodium for potassium does not alter their conductance or reversal potential. If the sodium permeability we assign to fiber-cell membranes is due to these channels, the methods described in this paper would not detect their potassium permeability. The evidence against a significant potassium permeability in fiber-cell membranes is: (*a*) If we calculate the passive leak of potassium that balances the measured rate of active transport (Mathias and Rae, 1985), then the measured value of surface-membrane conductance is sufficient to produce all of the passive leak. If there were significant potassium permeability in the fiber cells, then the leak would exceed the pump. (*b*) The measured radial gradients in steady-state voltages can be explained only if the fiber-cell membrane potassium selectivity is quite low (see the analysis by Mathias, 1985; or Mathias and Rae, 1985).

Sodium Permeability

The normal intracellular voltage for a frog lens is ~20 mV positive to E_K, which suggests that some 20% of the input conductance should be due to sodium selectivity. The conductance changes with sodium substitution reported here suggest there is a significant sodium permeability in the fiber-cell membranes. If roughly 50% of the fiber-cell membrane conductance is due to sodium selectivity, then we can account for the normal intracellular voltage as well as the spatial gradients in voltage reported in Mathias and Rae (1985). Moreover, the measured rate of active transport (Mathias and Rae, 1985) would just balance the passive leak through the fiber-cell membranes. Thus, general conclusions (*c*) and (*e*) of the Discussion fit nicely with several experimental observations, yet there are some reservations.

As mentioned in the Results, removal of sodium did not produce the expected hyperpolarization of the steady-state intracellular voltage. This was not due to changes in active transport, since it happened in the presence or absence of ouabain. One is therefore led to believe that there are channels that are gated in response to sodium removal, and these channels maintain the resting voltage at a constant value. If so, such channels would confuse our interpretation of conductance changes with sodium removal. Clearly, our sodium removal experiments produced confusing results concerning the conductance of surface-cell membranes, so maybe these observations fit together, but we are left with

very little reliable information on the amount of sodium permeability in surface-cell membranes.

Cell dissociation, whole-cell clamp, and patch-clamp studies (Rae, 1985) have not really clarified the situation, at least in the frog lens. The methods presently available for cell dissociation or decapsulation of the lens always cause some drop in input resistance and a depolarization of the intracellular voltage, thus one presumes new channels are being inserted or gated. Even so, the resting voltage of isolated cells from the frog lens epithelium is around −60 mV or within 30 mV of E_K, so one anticipates a dominance of potassium channels in the membranes. Yet in patch-clamp studies of these cells, one observes a dominance of nonselective cation channels, whose reversal potential is 0 mV. Furthermore, the frequency of these nonselective cation channels seems to increase as the day goes on and the cells deteriorate.

Patch clamp has, however, provided some clues to the sources of confusing results concerning sodium substitution experiments. The sodium substitutes TMA^+ or TEA^+ will both permeate the above mentioned nonselective cation channel, though much less easily than sodium, and this could be one cause of lens deterioration. Furthermore, there is a very large, totally nonselective channel (Fig. 11 of Rae and Levis, 1984), which is present in large numbers in virtually every patch from frog lens epithelial cells, but is normally not open. Among the various factors that will cause this channel to open is the combination of low calcium and substitution of either TMA^+ or TEA^+ for Na^+. This particular combination gates 10 to 20 channels per patch and reduces the membrane resistance to a few ohm cm^2. Though we have seen nothing quite so dramatic in our whole-lens studies, the gating of very few of these channels would cause significant increases in macroscopic conductance yet be difficult to study by patch clamp.

In summary, we have no direct information on the sodium permeability of normal surface cells. The nonselective cation channel or large nonselective channel observed in patch clamp studies (Rae and Levis, 1984; Rae, 1985) are good candidates as sources of confusing results. The cation channel may be gated or inserted in response to stress (such as sodium removal, cell isolation or patch clamping) but we do not know the frequency of occurrence in healthy, unstressed cells. The nonselective channel may be gated by sodium substitutes. The observed spatial gradients in steady-state voltages (Mathias and Rae, 1985) suggest that most of the sodium conductance resides in the membranes of fiber cells; the changes in conductance on sodium removal reported here are consistent with such a localization, hence, this is our present hypothesis.

Further Studies

The results reported here represent our first crude approximation to the localization of passive membrane properties in the lens. We hope to refine our description of the sites for passive permeability as well as for active transport. The most obvious experimental approaches of the future are cell isolation and patch clamp, but because of the reasons outlined in Rae (1985), these seemingly straightforward techniques may indeed be more difficult to interpret than the macroscopic approach described here. In general, patch clamp has been enormously valuable in providing a catalog of the building blocks that construct the macroscopic membrane permeability, but the frequency of occurrence of channels is equally important, and in this regard patch-clamp studies have not lived up to their promise. Hopefully, the future will bring improved understanding of these new techniques.

Some of the implications of the results presented here are examined in the accompanying paper (Mathias, 1985). Another approach to studying the localization of membrane properties is to devise experiments to test these implications. For example: (*a*) We have already followed this suggestion in our studies of the radial gradients in steady-state voltages (Mathias and Rae, 1985), which are one implication of the localization of transport reported here. (*b*) The vibrating probe, developed by Jaffe and Nuccitelli (1974), measures extracellular current flow and it has been used by Robinson and Patterson (1983) to demonstrate standing, steady-state current fluxes in the rat lens. An analysis of Robinson and Patterson's results in the context of our model has not been done, so we cannot say whether they are confirmatory or contradictory; nonetheless, these results clearly demonstrate the existence of standing, steady-state current loops. (*c*) The predicted radial circulation of sodium should produce an accompanying circulation of fluid and it seems feasible, at least in principle, to detect such a fluid flux, either directly or indirectly, by measuring the differences in diffusion, conduction, and convection of extracellular markers.

The experimental results presented in this paper and in the accompanying analysis have focused on the inner vs. surface properties of lens cell membranes and on the radial circulating fluxes that are generated by differences in these properties. Other investigators (Candia et al., 1971; Delamere and Duncan, 1979; Kinsey and Reddy, 1965; and Neville et al., 1978) have demonstrated differences in the anterior vs. posterior surface-cell membrane properties. Such differences will superimpose a net anterior/posterior flux of solute and fluid on the radial fluxes, hence our analysis and experimental techniques need to be extended to include surface-cell specializations. The complexity of normal lens electrophysiology far exceeds what one would have hypothesized ten years ago and the need to develop new techniques is clear.

We would like to thank Diane Mueller for recording Figs. 4 *B* and 6 *B* of this paper. We are also grateful to Dr. R. S. Eisenberg for a careful reading of the manuscript as well as many helpful discussions.

This work was supported by National Institutes of Health grants EY03095, EY03282, the Regenstein Foundation, and the Norton Trust (Chicago).

Received for publication 2 January 1985 and in final form 24 April 1985.

REFERENCES

Attwell, D., D. Eisner, and I. Cohen. 1979. Voltage clamp and tracer flux data: effects of a restricted extra-cellular space. *Quart. Revs. Biophys.* 12:213–261.

Benedetti, E. L., I. Dunia, C. J. Bentzel, A. J. M. Vermorken, M. Kibbelaar, and H. Bloemendal. 1976. A portrait of plasma membrane specializations in the eye lens epithelium and fibers. *Biochem. Biophys. Acta.* 457:353–384.

Candia, O. A., P. J. Bentley, and C. D. Mills. 1971. Short-circuit current and active Na transport across isolated lens of the toad. *Am. J. Physiol.* 220:558–563.

Delamere, N. A., and G. Duncan. 1979. The properties of bovine lens membranes measured by a conventional double-chamber method. *J. Physiol. (Lond.).* 295:241–249.

Delamere, N. A., C. A. Patterson, D. L. Holmes. 1980. The influence of external potassium ions upon lens conductance characteristics investigated using a voltage clamp technique. *Exp. Eye Res.* 31:651–658.

Duncan, G. 1970. Movement of sodium and chloride across amphibian lens membranes. *Exp. Eye Res.* 10:117–128.

Eisenberg, R. S., V. Barcilon, and R. T. Mathias. 1979. Electrical properties of spherical syncytia. *Biophys. J.* 25:151–180.

Fuchs, W., E. Hviid Larsen, and B. Lindemann. 1977. Current-voltage curve of sodium channels and concentration dependence of sodium permeability in frog skin. *J. Physiol. (Lond.).* 267:137–166.

Goodenough, D. A., J. S. B. Dick II, and J. E. Lyons. 1980. Lens metabolic cooperation: a study of mouse lens transport and permeability visualized with freeze-substitution autoradiography and electronmicroscopy. *J. Cell Biol.* 86:576–589.

Guerschanik, S. N., P. S. Reinach, and O. A. Candia. 1977. Chloride compartments of the frog lens and chloride permeability of its isolated surfaces. *Invest. Ophthalmol.* 16:512–520.

Hodgkin, A. L., and B. Katz. 1949. The effect of sodium ions on the electrical activity of the giant axon of the squid. *J. Physiol. (Lond.).* 108:37–77.

Jaffe, L. F., and R. Nuccitelli. 1974. An ultrasensitive vibrating probe for measuring steady extracellular current. *J. Cell Biol.* 63:614–628.

Johnson, E. A., and M. Lieberman. 1971. Heart: excitation and contraction. *Annu. Rev. Physiol.* 33:479–532.

Kinoshita, J. H. 1963. Selected topic in ophthalmic biochemistry. *Arch. Ophthalmol.* 70:558–573.

Kinsey, V. E., and D. V. N. Reddy. 1965. Studies of the crystalline lens XI. The relative role of the epithelium and capsule in transport. *Invest. Ophthal.* 4:104–116.

Mathias, R. T. 1985. Steady state voltages, ion fluxes and volume regulation in syncytial tissues. *Biophys. J.* 48:435–448.

Mathias, R. T., and J. L. Rae. 1985. Transport properties of the lens. *Am. J. Physiol.* In press.

Mathias, R. T., J. L. Rae, and R. S. Eisenberg. 1979. Electrical properties of structural components of the crystalline lens. *Biophys. J.* 25:181–201.

Mathias, R. T., J. L. Rae, and R. S. Eisenberg. 1981. The lens as a nonuniform spherical syncytium. *Biophys. J.* 34:61–83.

Neville, M. C., C. A. Patterson, and P. M. Hamilton. 1978. Evidence for two sodium pumps in the crystalline lens of the rabbit eye. *Exp. Eye Res.* 27:1–12.

Palva, M., and A. Palkama. 1974. Histochemically demonstrable sodium-potassium-activated adenosine triphosphatase (Na-K-ATPase) activity in the rat lens. *Exp. Eye Res.* 19:117–123.

Patterson, C. A., and B. A. Eck. 1971. Chloride concentrations and exchange in rabbit lens. *Exp. Eye Res.* 11:207–213.

Patterson, C. A., and D. M. Maurice. 1971. Diffusion of sodium in extracellular space of the crystalline lens. *Am. J. Physiol.* 220:256–263.

Patterson, C. A., M. C. Neville, R. M. Jenkins II, and D. K. Nordstrom. 1974. Intracellular potassium activity in frog lens determined using ion specific liquid ion-exchanger filled microelectrodes. *Exp. Eye Res.* 19:43–48.

Patmore, L., and G. Duncan. 1980. Voltage-dependent potassium channels in the amphibian lens membranes: Evidence from radiotracer and electrical conductance measurements. *Exp. Eye Res.* 31:637–650.

Platsch, K. D., and M. Wiederholt. 1981. Effect of ion substitution and ouabain on short circuit current in the isolated human and rabbit lens. *Exp. Eye Res.* 32:615–625.

Rae, J. L. 1974*a*. Potential profiles in the crystalline lens of the frog. *Exp. Eye Res.* 19:227–234.

Rae, J. L. 1974*b*. Voltage compartments in the lens. *Exp. Eye Res.* 19:235–242.

Rae, J. L. 1985. The application of patch clamp methods to ocular epithelia. *Current Eye Res.* 4:409–420.

Rae, J. L., and J. R. Kuszak. 1983. The electrical coupling of epithelium and fibers in the frog lens. *Exp. Eye Res.* 36:317–326.

Rae, J. L., and R. A. Levis. 1984. Patch voltage clamp of lens epithelial cells: theory and practice. *Molec. Physiol.* Elsevier/North-Holland, New York. 6:115–162.

Rae, J. L., and R. T. Mathias. 1984. The physiology of the lens. *In* The Lens. H. Maisel, editor. Marcel Dekker Inc., New York.

Rae, J. L., R. T. Mathias, and R. S. Eisenberg. 1982. Physiological role of the membranes and extracellular space within the ocular lens. *Exp. Eye Res.* 35:471–489.

Robinson, K. R., and J. W. Patterson. 1983. Localization of steady currents in the lens. *Curr. Eye Res.* 2:843–847.

Taura, Y., T. Murata, and N. Akaike. 1979. Topographical aspects of crystalline lens potential. *Comp. Biochem. Physiol.* 63A:475–480.